# H DIBARYON IN CHIRAL QUARK MODEL*

Z. DULIŃSKI

Dept. of Particle Physics, Jagellonian University
Reymonta 4, PL-30-059 Kraków, Poland

M. PRASZAŁOWICZ† AND P. SIEBER

Institut of Theor. Phys. II, Ruhr-University Bochum
D-4630 Bochum, Germany

*(Received October 20, 1993)*

The static energy of the baryon number $B = 2$ SO(3) soliton calculated within the framework of the Chiral Quark Model is interpreted as a mass of a dibaryon six quark state. The calculated mass is of the order of 3 GeV and therefore dilambda lies above the physical threshold for two $\Lambda$ decay. It is however argued that if the threshold itself is calculated within the same model dilambda mass is slightly below the mass of two $\Lambda$. This is due to the fact that the chiral models overestimate total masses usually by a few hundred MeV.

PACS numbers: 14.20. Pt

## 1. Introduction

In 1977 Jaffe [1] argued that within a framework of the MIT bag model a six-quark state uuddss (called H or dilambda) has a mass as low as 2.15 GeV and therefore is just below the two lambda threshold (2.23 GeV). If it was true H would have been stable against strong decays and could have been relatively easy seen in experiments [2–6]. Since that time there have been many calculations of H mass in various models (bag model [7–11], lattice QCD [12, 13], quark cluster model [14–17], Skyrme model [18–21] and non-relativistic quark model [22])with predictions ranging from 1.56 GeV to

* This work was partly sponsored by Polish Research Grant 2.0091.91.01 (Z.D. and M.P)

† Alexander von Humboldt Stiftung Fellow, on leave of absence from the Jagellonian University, Kraków, Poland

more than 3 GeV. In Ref. [23] dilamba mass was calculated in Chiral Quark Model ($\chi$QM) and it was found that $E_{\text{dilambda}} = 2.11$ GeV in the chiral limit. In the present paper we extend the calculations of Ref. [23] without the approximations employed in that work. We find that $E_{\text{dilambda}} \approx 2.5$ GeV in the chiral limit. Moreover we investigate in detail the dependence of this result on model parameters and discuss thoroughly the departure from the massless limit. The inclusion of the strange quark mass shifts $E_{\text{dilambda}}$ by approximately 0.5 GeV for the strange quark mass $m_s \approx 150$ MeV. Therefore the total mass of H is of the order of 3 GeV.

Although this result indicates that dilambda is unstable we can't have our beer and drink it. One has still to keep in mind that $\chi$QM *overestimates* baryon masses by a few hundred MeV. As we will argue later the model prediction for the two lambda threshold is always *above* the H mass. We are therefore confronted with a major problem, which is beyond the scope of this paper, namely the problem of understanding the predictions of the model as far as *total* masses are concerned.

It is widely believed that the low energy properties of QCD are reproduced by $\chi$QM in which constituent quarks are coupled in a chirally invariant way to pseudoscalar meson fields [24–31]. In our version of the model [27, 29, 30] pseudoscalars have no kinetic term and are treated as composite objects; one can view this model as a bosonized version of the quark Nambu–Jona-Lasinio (NJL) model [32]. Theoretically the model should be derivable from QCD. Indeed the instanton model of the QCD vacuum is believed to result in an effective theory of this kind [33, 34].

$\chi$QM being only an effective theory requires a cut-off. Throughout this paper we use proper time Schwinger regularization [35]. Regulator function is chosen in such a way that meson observables such as pion decay constant ($F_\pi = 93$ MeV) and pseudoscalar masses (or equivalently quark condensate $\langle\overline{\psi}\psi\rangle = -(239\text{ MeV})^3$ ) are reproduced. The details can be found in Refs [27–30], [36–38]. It is important to note that the model reproduces very well pion scattering amplitudes [39], or, in other words, Gasser-Leutweyler coefficients [40].

While mesonic properties are calculated by integrating out the quark fields and by expanding the effective action in terms of the derivatives of the pseudoscalars, the baryonic properties are evaluated by assuming that the pseudoscalar fields are topologically non-trivial. It is convenient to parametrize the mesonic fields in terms of an SU(3) matrix:

$$U[\phi_i] = \exp\left(i\frac{\vec{\lambda}\cdot\vec{\phi}}{F_\pi}\right), \tag{1.1}$$

where $\lambda_i$ are Gell-Mann SU(3) matrices and $\phi_i$ correspond to the pseudoscalar fields ($i = 1, \ldots, 8$). For the nucleon, or in general for ordinary

baryons, the topologically non-trivial configuration means that [41, 42]:

$$\phi_i = n_i F_\pi P(r) \quad \text{for} \quad i = 1,2,3\,,$$
$$\phi_i = 0 \quad \text{for} \quad i = 4,\ldots,8, \tag{1.2}$$

where $n_i$ denotes a unit vector, and $P(r)$ is a function of a radial distance only. $P$ obeys certain boundary conditions at $r = 0$ and $r \to \infty$, but otherwise is free, and one finds its precise shape by minimizing the energy of a valence level and continuum levels regularized in an appropriate way. In recent papers Blotz *et al.* [43, 44] showed that the mass splittings of the ordinary baryons are reproduced with an accuracy of a few MeV. This encouraging result is however spoiled by the fact that *absolute* masses are overestimated by about 400 MeV — this is a common feature of all chiral models [45]. We will come back to this point in Sections 4 and 5.

Balachandran *et al.* proposed, in the context of the Skyrme model, another classical Ansatz for $U$ [18, 19]:

$$U[f,g] = \exp\left(i\,\vec{n}\cdot\vec{\Lambda}\,f(r) + i\left[(\vec{n}\cdot\vec{\Lambda})^2 - \tfrac{2}{3}\right] g(r)\right), \tag{1.3}$$

where $\vec{\Lambda} = (\lambda_5,\ -\lambda_2,\ \lambda_7)$ and $\vec{n}$ is a unit vector. Matrices $\Lambda_i$ generate an SO(3) subgroup of the SU(3) flavor group. To make $U$ well-defined at the origin one has to impose the following boundary conditions on functions $f$ and $g$:

$$f(0) = n\pi \quad \text{and} \quad g(0) = \pm m\pi, \qquad m,n = 1,2\ldots. \tag{1.4}$$

The topological number of Ansatz (1.3), which in the Skyrme model is identified with the baryon number, is equal to $B = 2\,f(0)/\pi$; therefore the lowest possible baryon number generated by (1.3) is 2.

In Ref. [23] the energy of Ansatz (1.3) was calculated for constituent quark mass $M = 345$ MeV. In order to evaluate the continuum part an approximation based on so called *interpolation formula* was employed. In this paper we calculate the energy of the sea exactly, we also calculate H mass for various constituent quark masses and for different bare strange quark mass $m_s$.

Here an important remark concerning the parity of the H particle is in order. Ansatz (1.3) has no definite behavior under the parity transformation:

$$U(\vec{r}) \to U^\dagger(-\vec{r}) \neq \pm U(\vec{r})\,. \tag{1.5}$$

The parity transformation corresponds to a replacement $g \to -g$. Therefore, classically, the parity P=+1 and P = −1 states are degenerate. However,

since two Ansätze $U^{(1,2)}$ (corresponding to $g_1 = g$ and $g_2 = -g$ respectively) have the same topological number $B$, there should exist a family of interpolating Ansätze $U^{\text{int}}(\tau)$, where $\tau \in (-\infty, \infty)$, such that [23]:

$$U^{\text{int}}(-\infty) = U^{(1)} \quad \text{and} \quad U^{\text{int}}(\infty) = U^{(2)}. \tag{1.6}$$

One could in principle calculate the action corresponding to the transition from $U^{(1)} \to U^{(2)}$ and, in this way, estimate the splitting of P=+1 and P = −1 states. In any case this splitting will be parametrically small, *i.e.* of the order $\exp(-N_c)$.

Assuming that $U$ is of the form (1.3), we study the spectrum of the quark Dirac hamiltonian in the presence of such configuration and develop techniques to sum up the contribution of the continuum energies – vacuum polarization. We observe that the continuum energy *increases* almost linearly with suitably defined size of the soliton field. In the same time two degenerate valence levels, with 3 (or $N_c$) quarks each emerge from upper continuum. Their energy *decreases* with the soliton size. The sum of the two contributions: *valence* + *continuum* develops a stable minimum which we interpret as a dilambda mass.

In Section 2 we briefly describe the formalism. Since in the literature there exist detailed descriptions of the model and numerical method [27, 29, 30, 37, 38], here we only recapitulate main points and set our notation. In Section 3 we present our results for $m_s = 0$. We find that for constituent masses smaller that 325 MeV there is no stable solitonic solution; in this respect the situation is analogous to the nucleon case, where no solutions were found for this range of constituent masses as well. $E_{\text{dilambda}}$ decreases with increasing $M$. In Section 4 we discuss the departure from the chiral limit. First we calculate the analog of the nucleon sigma commutator and calculate the energy shift due to the non-zero strange quark mass in a linear approximation. This shift, as already observed in Ref. [23] is as large as 1 Gev (600 MeV) for the constituent mass of 350 MeV (600 MeV) and $m_s = 156$ MeV. Therefore the linear approximation is not reliable. Next we calculate the energy shift in an approximation where the singlet part of the mass matrix is treated exactly and find that it varies from 600 to 500 MeV for constituent masses $M = 350$ to 600 MeV. Our final conclusions are presented in Section 5, where we also compare our results with the results of Refs [43, 44] where masses of hyperons were calculated.

## 2. Dilambda in chiral quark model

In $\chi$QM model the problem of calculating the energy of a classical field configuration given in terms of an $N_f \times N_f$ matrix $U[\phi_i(\vec{r})]$ parametrized

by $n$ functions $\phi_i$, $(i = 1, \ldots, n)$ consists in finding a minimum with respect to $\phi_i$ of a functional:

$$E = \min_{\phi_i} \left( E_{\text{level}}[\phi_i] + E_{\text{cont.}}[\phi_i] \right). \tag{2.1}$$

Quantities $E_{\text{level}}$ and $E_{\text{cont.}}$ are constructed in terms of eigenenergies of the one-particle Dirac hamiltonian:

$$\gamma_0 \left( -i\gamma_k \frac{\partial}{\partial r_k} + M \left( U[\phi_i] \frac{1+\gamma_5}{2} + U^\dagger[\phi_i] \frac{1-\gamma_5}{2} \right) + m \right) \psi_l = M \epsilon_l[\phi_i] \psi_l , \tag{2.2}$$

where $M$ stands for constituent quark mass and $m$ denotes bare quark mass matrix. In this notation we have:

$$E_{\text{level}}[\phi_i] = N_c M \sum_{l \in \text{valence}} \epsilon_l[\phi_i] , \tag{2.3}$$

$$E_{\text{cont.}}[\phi_i] = N_c M \sum_{l \in \text{continuum}} \left( R(\epsilon_l[\phi_i]) - R(\epsilon_l[0]) \right). \tag{2.4}$$

Here subscripts "valence" and "continuum" refer to valence levels with energies $0 < \epsilon_l < 1$ and to *all* levels respectively, $\phi_i \equiv 0$ correspond to the vacuum configuration. Throughout this paper we use the proper time regularization:

$$R(\epsilon) = \frac{1}{4\sqrt{\pi}} \int_0^\infty \frac{d\tau}{\tau^{3/2}} \varphi(\tau) e^{-\epsilon^2 \tau} , \tag{2.5}$$

where a step-like function $\varphi(\tau)$ is a subject to two conditions:

$$\frac{N_c M^2}{4\pi^2} \int_0^\infty \frac{d\tau}{\tau} \varphi(\tau) e^{-\tau} = F_\pi^2 , \tag{2.6}$$

$$\frac{N_c M^3}{4\pi^2} \int_0^\infty \frac{d\tau}{\tau^2} \varphi(\tau) e^{-\tau} = -\langle \bar{\psi}\psi \rangle , \tag{2.7}$$

with $F_\pi = 93$ MeV and the quark condensate $\langle \bar{\psi}\psi \rangle = -(239\,\text{MeV})^3$. With this value of the quark condensate the strange quark mass which reproduces the kaon mass (in gradient expansion) is:

$$m_s = 156 \ \text{MeV} . \tag{2.8}$$

Let us remark that in contrast to $E_{\text{dilambda}}$ the value of the sigma term (in ordinary baryon case and in our case as well) depends drastically on the fact

whether condition (2.7) is satisfied or not. The hyperon splittings, which depend on the sigma commutator, have been successfully reproduced with the two step cut-off function saturating conditions (2.6) *and* (2.7) simultaneously [43, 44].

The above formulae can be applied to any classical field configuration $U$. Following Refs [18, 19] and Ref. [23] we choose $U$ in a form given by Eq. (1.3) which can be conveniently rewritten as:

$$U_{kl}[f,g] = \exp\left(i\frac{g}{3}\right)\left(\delta_{kl}\cos f + n_k n_l(\mathrm{e}^{-ig} - \cos f) + \varepsilon_{klm}n_m \sin f\right), \tag{2.9}$$

where $k,l = 1,2,3$.

Functions $f$ and $g$ depend only on the radial distance $r$ and are chosen to obey boundary conditions [18–20]:

$$\begin{aligned} f(0) &= \pi \quad \text{and} \quad f(r\to\infty) \sim \frac{1}{r^2}, \\ g(0) &= \pm\pi \quad \text{and} \quad g(r\to\infty) \sim \frac{1}{r^3}. \end{aligned} \tag{2.10}$$

As seen from the form of Ansatz (2.9) hamiltonian (2.2) has a *generalized* rotational symmetry corresponding to the grand-spin operator $\boldsymbol{K}$:

$$\boldsymbol{K} = \boldsymbol{\Lambda} + \boldsymbol{L} + \boldsymbol{S}, \tag{2.11}$$

where $\boldsymbol{\Lambda}$ denotes the SO(3) symmetry operator ($\Lambda = 1$), $\boldsymbol{J}$ is the ordinary angular momentum operator ($J = 0,1,\ldots$) and $\boldsymbol{S}$ stands for spin ($S = {}^1/_2$). Therefore $K = {}^1/_2, {}^3/_2, \ldots$. We can diagonalize the angular part of the hamiltonian (2.2) by writing a general solution to the Dirac equation (2.2) with Ansatz (2.9) as:

$$\psi_{K K_3}(\vec{r}) = \begin{bmatrix} \sum\limits_{ij} F^K_{(i,j)}(r)\, \Xi^{(i,j)}_{K K_3}(\vec{n}) \\ -i \sum\limits_{ij} G^K_{(i,j)}(r)\, \Xi^{(i,j)}_{K K_3}(\vec{n}) \end{bmatrix}, \tag{2.12}$$

where the flavor-spinors $\Xi^{(i,j)}_{K K_3}$ can be found in Appendix A. For each $K$ Eq. (2.2) reduces to 12 first-order differential equations for 12 radial functions $F^K_{(i,j)}(r)$ and $G^K_{(i,j)}(r)$ ($i = \pm, 0$ and $j = \pm$). In fact, for $K = {}^1/_2$ the system reduces to 8 equations ($i = -$ does not contribute).

Let us remark here, that since $U[f,g]$ does not transform into itself under the parity transformation, parity is *not* a good quantum number here, and — unlike in the nucleon case — the 12 (or 8 for $K = {}^1/_2$) equations do

not split into two subsets of 6 (or 4) differential equations, one for parity $+1$ and one for parity $-1$.

It is convenient to define a 12 component vector $\Psi_{K,n}(x)$ and rewrite Eq. (2.2) in the following form:

$$\left(N\frac{d}{dx}+\frac{1}{x}C_K+H_K[f,g]\right)\Psi_{K,n}(x)=\epsilon_{K,n}[f,g]\,\Psi_{K,n}(x), \tag{2.13}$$

where $12\times 12$ matrices $N$, $C_K$ and $H_K$ as well as $\Psi_{K,n}$ are explicitly given in Appendix B; $x\equiv Mr$ and $n$ enumerates subsequent energy levels. In what follows we will suppress index $n$.

Instead of performing a full-scale selfconsistent minimization of the energy functional (2.1) we use a variational approach and minimize (2.1) with respect to two variational parameters: $r_f$ and $r_g$ defined as in Ref. [23]:

$$f=2\arctan\left(\frac{r_f}{r}\right)^2, \qquad g=2\arctan\left(\frac{r_g}{r}\right)^3. \tag{2.14}$$

The variation method proved to be very accurate in the nucleon case [36].

The numerical method used to calculate single particle energy levels $\epsilon_K$ is analogous to the one described in Refs [25, 29, 30] in the context of the nucleon solution. The idea is to construct a convenient, finite (but large enough) $n$ dimensional basis in which $12\times 12$ matrices of Eq. (2.13) are transformed into $n\times n$ component matrices, which are subsequently numerically diagonalized. The size of the basis should be chosen in such a way that numerical stability with respect to the change of $n$ is achieved.

In order to construct the basis let us first observe that in the absence of the soliton (*i.e.* $f=g=0$), or for large $x$, the solution of Eq. (2.13) reduces to certain combination of the spherical Bessel functions. It is therefore natural to choose the 12 basis vectors in the following form:

$$\Phi_K^{(i)}=\begin{bmatrix}0\\ \vdots\\ j_{\nu(K,i)}(kx)\\ \vdots\\ 0\end{bmatrix}\leftarrow i, \tag{2.15}$$

where index $\nu$ is equal to the index of the Bessel function in the $i$-th entry ($i=1,\ldots,12$) of the free solution. The details can be found in Appendix C. Here

$$k=\sqrt{|\epsilon^2-1|}. \tag{2.16}$$

In the dilambda case the free equation (2.13) splits into three independent sets of 4 equations since matrices $N$, $C_K$ and $H_K$ become block diagonal, for instance:

$$H_K = \begin{bmatrix} H_K^{(+,+)} & 0 & 0 \\ 0 & H_K^{(0,0)} & 0 \\ 0 & 0 & H_K^{(-,-)} \end{bmatrix}. \tag{2.17}$$

The basis (2.15) corresponds to the continuous spectrum of Eq. (2.13). In order to discretize the energy levels, we close the system in a large box of radius $D$ and impose three separate boundary condition for each $4 \times 4$ subsystem independently:

$$j_{K-\frac{1}{2}+j}(k_i^j D) = 0\,, \qquad j = \pm 1,\ 0 \tag{2.18}$$

and index $i$ enumerates subsequent solutions to Eq. (2.18). Here comes the difference with the nucleon case, where one usually imposes one boundary condition for the whole system.

Equation (2.18) has an infinite number of solutions for $k$: $i = 1, 2, \ldots$. For practical purposes we have to work with a finite basis, which we define by choosing a cut-off:

$$k_i^{\pm 0} < k_{\max}. \tag{2.19}$$

Equation (2.19) generates 3 sets of solutions. There are $n_+$ solutions in the first set, and $n_0$ and $n_-$ solutions in the remaining two. Therefore the size of the basis is equal:

$$n = 4\,(n_+ + n_0 + n_-)\,.$$

With $k$ satisfying Eqs (2.18), (2.19) each one of 12 vectors (2.15) transforms into $n_+$, $n_0$ or $n_-$ vectors which span our basis.

Next we calculate matrix elements of operators $N\,d/dx$, $C_K/x$ and $H_K$ in this basis and then diagonalize the hamiltonian (2.13). In this way we obtain the eigenvalues needed to calculate the energy of the soliton (see Eqs (2.3), (2.4)). One has of course to make sure that numerical stability with respect to $k_{\max}$ and $D$ is achieved.

## 3. Dilambda mass in chiral limit

Firstly we have to specify the cut-off function $\varphi(\tau)$ in order to satisfy conditions (2.6) and (2.7) — we call this a physical cut-off. We will show that our results do not depend on the specific choice of $\varphi(\tau)$ once the requirements (2.6) and (2.7) are fulfilled. Next we have to specify unphysical

cut-off parameters, namely $D$ and $k_{\max}$. They have to be chosen big enough so that the numerical stability against changes of $D$ and $k_{\max}$ is achieved. In practice we choose:

$$D = \frac{10}{M}, \qquad k_{\max} = 9\,M. \tag{3.1}$$

Let us illustrate the independence of our results on different ways of choosing the cut-off parameters on the example of the constituent mass $M = 400$ MeV. The results for other masses are similar. In order to satisfy conditions (2.6) and (2.7) we choose, as in Refs [43, 44] the cut-off function $\varphi(\tau)$ in a form of a two-step function:

$$\varphi(\tau) = (1-c)\,\Theta(\tau - \tau_1) + c\,\Theta(\tau - \tau_2) \tag{3.2}$$

with

$$\tau_i \equiv \left(\frac{M}{\Lambda_i}\right)^2. \tag{3.3}$$

TABLE I

Dependence of energy and sigma-term on the physical cut-off.

| $\Lambda_1/M$ | $\Lambda_2/M$ | $c$ | $E_{\text{valence}}$ [GeV] | $E_{\text{cont.}}$ [GeV] | $E$ [GeV] | $\sigma_{\text{valence}}$ | $\sigma_{\text{cont.}}$ | $\sigma$ |
|---|---|---|---|---|---|---|---|---|
| 0.65 | 3.2 | 0.376 | 1.03 | 1.41 | 2.45 | 1.03 | 5.02 | 6.04 |
| 0.78 | 3.3 | 0.346 | 1.03 | 1.43 | 2.46 | 1.03 | 4.96 | 5.98 |
| 0.87 | 3.4 | 0.319 | 1.03 | 1.43 | 2.47 | 1.03 | 4.92 | 5.95 |
| 0.98 | 3.6 | 0.272 | 1.03 | 1.43 | 2.47 | 1.03 | 4.88 | 5.81 |
| 1.06 | 3.8 | 0.234 | 1.03 | 1.43 | 2.47 | 1.03 | 4.85 | 5.87 |
| 1.12 | 4.0 | 0.203 | 1.03 | 1.43 | 2.47 | 1.03 | 4.82 | 5.85 |
| 1.23 | 4.5 | 0.147 | 1.03 | 1.43 | 2.47 | 1.03 | 4.76 | 5.79 |
| 1.30 | 5.0 | 0.111 | 1.03 | 1.44 | 2.47 | 1.03 | 4.69 | 5.72 |

In Table I we display the value of the minimum of $E_{\text{dilambda}}$ for $D = 10/M$ and $k_{\max} = 9\,M$ for various choices of $\Lambda_1$, $\Lambda_2$ and $c$. For $\Lambda_2 < 3.2\,M$ no solution to the conditions (2.6) and (2.7) was found. The contributions of the valence level and continuum are separately displayed, the last three columns refer to the sigma term which we discuss in the next section. We see from Table I that the minimum energy $E$, which we interpret as a dilambda mass, is fairly independent upon the choice of the cut-off parameters. In Fig. 1 we plot the dependence of the total energy $E$ on $\Lambda_2$; $\Lambda_1$ and $c$ are fixed by conditions (2.6) and (2.7) and can be read out from Table I. On the same plot, for comparison, we display the value of $E$ for $c = 0$, *i.e.* for one-step cut-off function which reproduces $F_\pi$ but *not* the condensate. One

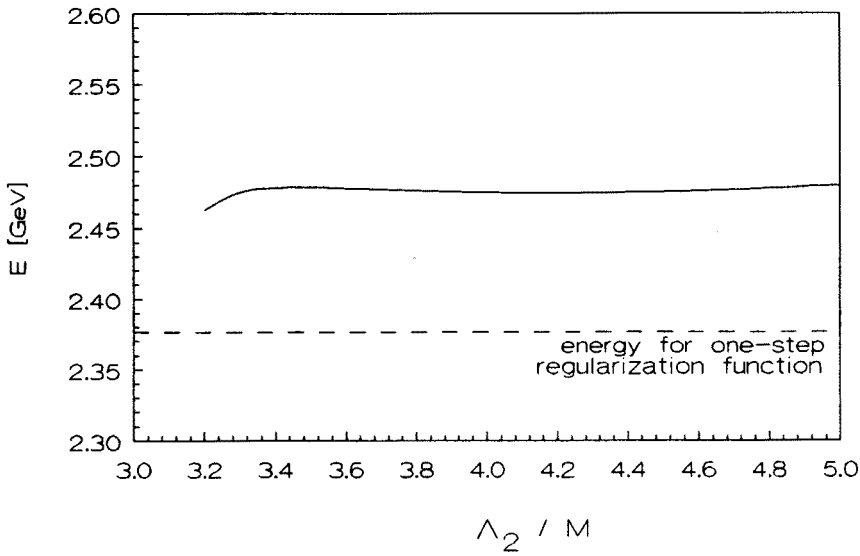


Fig. 1. Dependence of $E$ on cut-off parameter $\Lambda_2$ with $\Lambda_1$ and $c$ fixed by conditions (2.6) and (2.7). Dashed line corresponds to energy $E$ calculated with $c = 1$.

can see that even for this simplified cut-off the energy is lower only by 0.1 GeV (*i.e.* 4 %) with respect to the two-step cut-off.

In the remainder of this paper, following Refs [43, 44], we restrict ourselves to the choice:

$$\Lambda_1 = 0.87\,M, \quad \Lambda_2 = 3.4\,M, \quad c = 0.319\,. \tag{3.4}$$

With cut-off parameters fixed by Eq. (3.4) we now investigate the dependence of our results upon the choice of $D$ and $k_{\max}$. In Table II we present the results for energies and sigma terms for 3 various choices of $D$ and $k_{\max}$. Again we found almost no dependence on $D$ and $k_{\max}$. With our parameters fixed by equations (3.4) and (3.1) we can now study the dependence of H mass on the constituent mass $M$ with $m_s = 0$. Our results are summarized in Table III.

TABLE II

Dependence of energy and sigma-term on $D$ and $k_{\max}$.

| $D\,M$ | $k_{\max}/M$ | $E_{\text{valence}}$ [GeV] | $E_{\text{cont.}}$ [GeV] | $E$ [GeV] | $\sigma_{\text{valence}}$ | $\sigma_{\text{cont.}}$ | $\sigma$ |
|---|---|---|---|---|---|---|---|
| 10.0 | 9.0 | 1.03 | 1.43 | 2.47 | 1.03 | 4.92 | 5.95 |
| 10.0 | 12.0 | 1.03 | 1.43 | 2.46 | 1.03 | 4.92 | 5.95 |
| 13.0 | 9.0 | 1.03 | 1.43 | 2.47 | 1.03 | 5.05 | 6.07 |

Similarly to the nucleon case H consists of a valence level and continuum levels which contribute via Eq. (2.1) to its mass. For zero-size soliton (*i.e.* $r_f = r_g = 0$) the spectrum of the hamiltonian (2.13) is symmetric and there are no levels in a mass gap $-1 < \epsilon < 1$. As soon as we slowly increase $r_f$ and $r_g$ the energy levels move and the spectrum is no longer symmetric. Moreover, due to the index theorem, a doubly degenerate $K = {}^1/_2$ level starting from some critical values of $r_f$ and $r_g$ crosses the $\epsilon = 1$ line and dives fast towards the lower continuum. In our model this level is filled with $N_c$ (*i.e.* 3) quarks, but due to $K_3$ degeneracy we have altogether $2N_c$ (*i.e.* 6) valence quarks, whose energy decreases rapidly with an increase of the soliton size. At the same time the energy of the continuum increases, but not as fast as the valence quarks energy, and for some value of the soliton size the minimum is achieved. For higher values of $r_f$ and $r_g$ the growth of the continuum energy wins over the decrease of the valence levels and the total energy increases with the soliton size.

TABLE III

Dilambda energy and $\sigma$-term for various constituent masses $M$ and strange quark masses $m_s$.

| $M$ [MeV] | $m_s$ [MeV] | $r_f M$ | $r_g M$ | $\sigma$ | $E$ [GeV] | |
|---|---|---|---|---|---|---|
| | | | | | linear | nonlinear |
| 325 | 0 | 0.8 | 0.9 | 4.90 | 2.56 | 2.56 |
| | 50 | – | – | | 2.81 | – |
| | 100 | – | – | | 3.05 | – |
| | 156 | – | – | | 3.32 | – |
| | 200 | – | – | | 3.54 | – |
| 350 | 0 | 1.0 | 1.1 | 6.93 | 2.48 | 2.48 |
| | 50 | 0.9 | 1.0 | | 2.83 | 2.72 |
| | 100 | 0.9 | 0.9 | | 3.18 | 2.89 |
| | 156 | 0.8 | 0.8 | | 3.56 | 3.03 |
| | 200 | 0.8 | 0.8 | | 3.86 | 3.13 |
| 400 | 0 | 1.1 | 1.2 | 5.95 | 2.47 | 2.47 |
| | 50 | 1.0 | 1.2 | | 2.76 | 2.68 |
| | 100 | 1.1 | 1.2 | | 3.06 | 2.84 |
| | 156 | 1.1 | 1.2 | | 3.40 | 2.99 |
| | 200 | 1.1 | 1.2 | | 3.66 | 3.10 |
| 500 | 0 | 1.3 | 1.5 | 4.95 | 2.39 | 2.39 |
| | 50 | 1.3 | 1.5 | | 2.64 | 2.59 |
| | 100 | 1.3 | 1.5 | | 2.89 | 2.73 |
| | 156 | 1.3 | 1.5 | | 3.16 | 2.86 |
| | 200 | 1.4 | 1.5 | | 3.38 | 2.96 |
| 600 | 0 | 1.4 | 1.7 | 3.67 | 2.32 | 2.32 |
| | 50 | 1.5 | 1.7 | | 2.51 | 2.49 |
| | 100 | 1.5 | 1.8 | | 2.69 | 2.61 |
| | 156 | 1.5 | 1.8 | | 2.90 | 2.74 |
| | 200 | 1.6 | 1.8 | | 3.06 | 2.82 |

For $M < 325$ MeV we find no minimum of the energy (2.1) with respect to parameters $r_f$ and $r_g$. For $M \geq 325$ MeV the minimum exists and the energy in the minimum decreases with an increasing M. The minima are rather shallow and the energy splits in almost equal portions between valence and the continuum part. In Fig. 2 we display the dependence of $E$ on $r_f$ ($r_g$) for $r_g$ ($r_f$) fixed to the position of the minimum (see Table III). The dashed line $E/M = 6$ corresponds to the free quark threshold. For $M > 400$ MeV the minima are below the free quark threshold.

Let us remark here that $\chi$QM does not incorporate confinement, therefore the free quark asymptotic states are in principle possible. Hence it is clear that we cannot trust the model at small distances, *i.e.* the model certainly breaks down for soliton sizes too small. Fortunately the minima are achieved for reasonably large $r_f$ and $r_g$. If the energy of the minimum is above the 6 quark threshold the system could in principle tunnel to a free quark quantum state, this however requires the soliton to squeeze to zero-size where confinement effects become important and $\chi$QM is not applicable. But even within the framework of the model this amplitude is parametrically small as it behaves like $\exp(-N_c)$. Let us finish by a remark that in order to reproduce the hyperon splittings the constituent mass has to be slightly larger than 400 MeV [43, 44]. For this range of $M$ the energy of dilambda is just below the free quark threshold.

## 4. Finite strange quark mass

So far we have been working in the chiral limit. Now we will discuss the inclusion of the finite mass of the strange quark. We will however, for simplicity, keep the up and down quark massless. The bare quark matrix $m$=diag(0,0,$m_s$) takes a form:

$$m = \tfrac{1}{3} m_s (1 - \sqrt{3}\,\lambda_8)\,. \tag{4.1}$$

Since H is a flavor singlet only a piece proportional to 1 contributes to the H mass.

For $m_s$ not too small the energy shift due to the strange quark mass can be expressed in terms of a Taylor expansion:

$$E = E(m_s = 0) + m_s \left(\frac{\partial E}{\partial m_s}\right)_{m_s=0}. \tag{4.2}$$

Let us define the energy shift due to the non-zero $m_s$ as:

$$\Delta E = \sigma m_s\,, \tag{4.3}$$

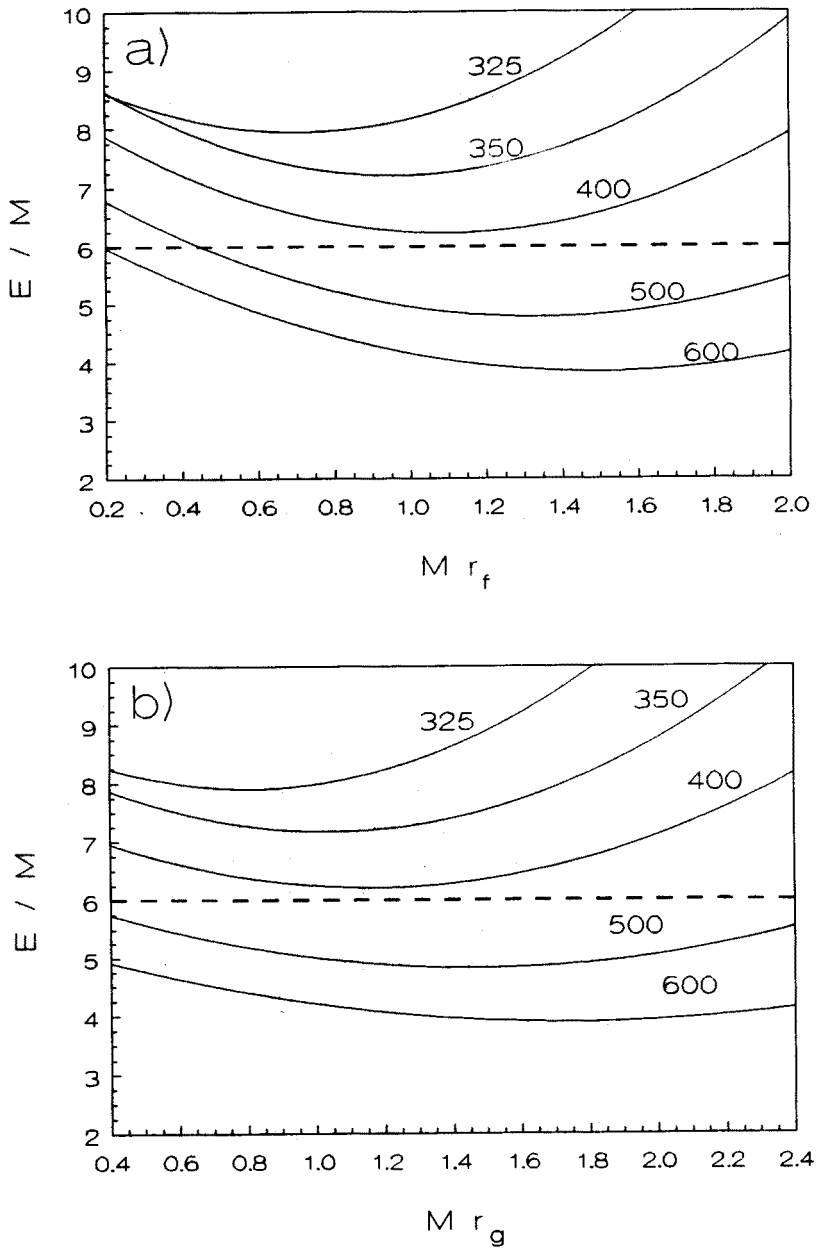


**Fig. 2. Dependence of $E$ (in units of $M$) on variational parameters $r_f$ (a) and $r_g$ (b) (in units $1/M$) for different constituent masses $M$. Dashed line corresponds to a six-quark threshold.**

where $\sigma$ is just the derivative explicitly displayed in Eq. (4.2).

We have calculated $\sigma$ in three different ways. Firstly, we have inserted (4.1) in the hamiltonian (2.2) and calculated the derivative $\sigma$ numerically. Secondly we have used the formula, which expresses $\sigma$ in terms of the quark wave functions:

$$\sigma = \sigma_{\text{valence}} + \sigma_{\text{cont.}}, \tag{4.4}$$

where

$$\sigma_{\text{cont.}} = \frac{N_c}{3} \sum_{l \in \text{continuum}} \left[ \langle \psi_l \mid \gamma_0 \mid \psi_l \rangle \left( \frac{dR}{d\epsilon} \right)_{\epsilon=\epsilon_l[\phi_i]} - \frac{1}{\epsilon_l[0]} \left( \frac{dR}{d\epsilon} \right)_{\epsilon=\epsilon_l[0]} \right]$$

$$\sigma_{\text{valence}} = \frac{N_c}{3} \sum_{l \in \text{valence}} \langle \psi_l \mid \gamma_0 \mid \psi_l \rangle \,. \tag{4.5}$$

Here $\psi_l$ are solutions of Eq. (2.2). Thirdly, we have used gradient expansion [45]:

$$\sigma_{\text{cont.}} = -4\pi \frac{\langle \bar{\psi}\psi \rangle}{M^3} \int dr\, r^2 \left( 3 - 2\cos f \cos \frac{g}{3} - \cos \frac{2g}{3} \right). \tag{4.6}$$

All three methods give the same result. In the fifth column of Table III we display the values of $\sigma$ for different constituent masses.

Before we discuss the physical consequences of expansion (4.2) let us note that results for $\sigma$ are basically insensitive to the choice of cut-off parameters. In Tables I and II the values of $\sigma_{\text{valence}}$, $\sigma_{\text{cont.}}$ and $\sigma$ are displayed for different physical and unphysical cut-off parameters. The slight variation of $\sigma$ with respect to $\Lambda_2$ is illustrated in Figure 3.

In Figure 4 we plot $\Delta E$ as a function of $m_s$ in the linear approximation (straight lines) for two extreme choices of the constituent mass $M = 350$ MeV and $M = 600$ MeV. The smaller the constituent mass the bigger $\Delta E$. Certainly the shift of 1 GeV in comparison to the chiral limit result of the order of 2.5 GeV cannot be considered as small. We are therefore led to the conclusion that $m_s$ should be, at least in the case of dilambda, treated non-linearly.

It is obvious that for finite $m_s$ some nonlinearities which will invalidate the linear approximation used so far must occur. In order to estimate these nonlinearities we will not expand $E$ in a power series in $m_s$. Instead, we will keep the singlet part of (4.1) in the hamiltonian (2.2) and minimize $E$ with respect to $r_f$ and $r_g$. However, one cannot forget that asymptotics (2.10) is no longer correct. For finite $m_s$ the profile functions are exponentially dumped for $r \to \infty$. Therefore instead of Ansätze (2.14) we take our profile

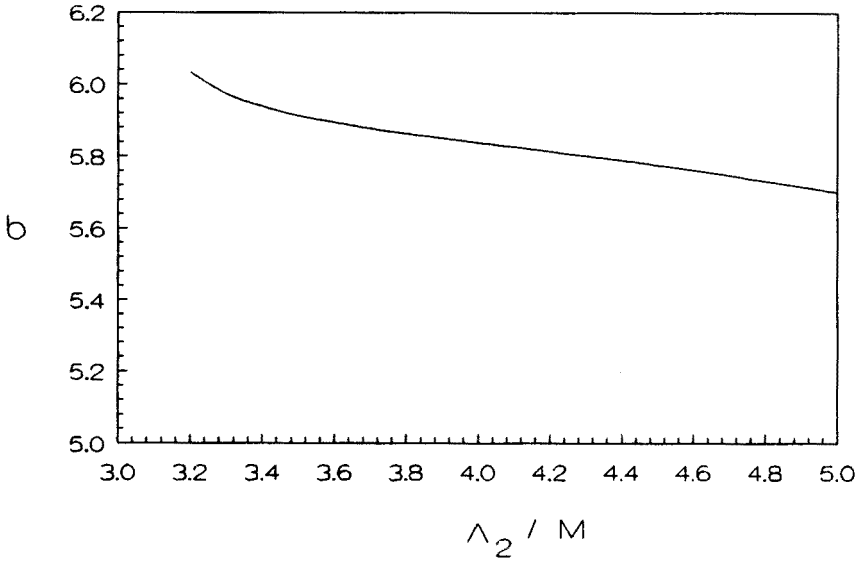


Fig. 3. $\sigma$ dependence on cut-off parameter $\Lambda_2$ with $\Lambda_1$ and $c$ fixed by conditions (2.6) and (2.7).

functions in the following form:

$$f = 2 \arctan\left(\frac{r_f}{r}\right)^2 \left[e^{-\mu r}(1+\mu r)\right] ,$$
$$g = 2 \arctan\left(\frac{r_g}{r}\right)^3 \left[e^{-\mu r}\left(1+\mu r+\frac{1}{3}(\mu r)^2\right)\right] , \qquad (4.7)$$

where $\mu$ is related to $m_s$:

$$\mu^2 = -\frac{2}{3} m_s \frac{\langle\bar{\psi}\psi\rangle}{F_\pi^2} . \qquad (4.8)$$

We have performed minimization of $E$ with $m_s$ included in the Hamiltonian (2.2) for both Ansätze: "non-exponential" (2.14) and "exponential" (4.7). The results, for $M = 400$ MeV are given in Table IV.

We also illustrate the difference between "non-exponential" (2.14) and "exponential" (4.7) parametrizations of trial functions $f$ and $g$ in Fig. 5, where the mass of dilambda is plotted against $m_s$ for constituent quark mass $M = 400$ MeV. In Fig. 5 we also plot the linear approximation given by Eq. (4.2). It can be seen that a degree of nonlinearity is much higher for "exponential" Ansätze (4.7). For physical strange quark mass $m_s = 156$ MeV the linear and "non-exponential" parametrizations overestimate $E$ by about 400 to 300 MeV.

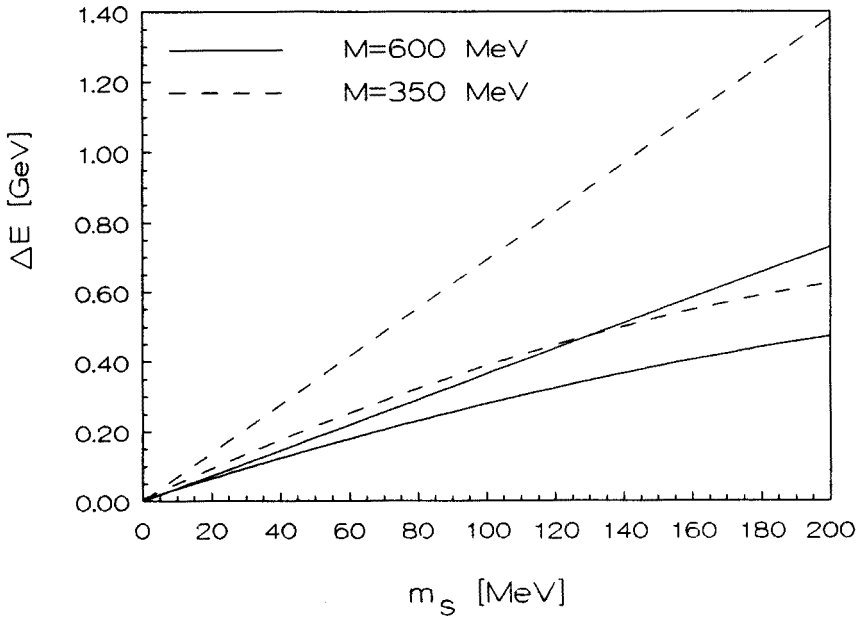


Fig. 4. $\Delta E$ dependence on $m_s$ for two constituent masses $M = 350$ MeV (dashed line) and $M = 600$ MeV (solid line). Upper straight lines correspond in both cases to linear approximation (4.3), while lower convex lines correspond to exact $m_s$ dependence, evaluated with "exponential" parametrization (4.7).

TABLE IV

Energy of H calculated with two different profiles for $M = 400$ MeV.

| | Profile Eq. (4.7) (exponential) | | | Profile Eq. (2.14) (non-exponential) | | |
|---|---|---|---|---|---|---|
| $m_s$ [MeV] | $E_{\text{valence}}$ [GeV] | $E_{\text{cont.}}$ [GeV] | $E$ [GeV] | $E_{\text{valence}}$ [GeV] | $E_{\text{cont.}}$ [GeV] | $E$ [GeV] |
| 50 | 1.31 | 1.37 | 2.68 | 1.09 | 1.67 | 2.76 |
| 100 | 1.51 | 1.32 | 2.84 | 1.14 | 1.91 | 3.05 |
| 156 | 1.71 | 1.28 | 2.99 | 1.20 | 2.16 | 3.36 |
| 200 | 1.86 | 1.24 | 3.10 | 1.25 | 2.35 | 3.60 |

It is interesting to observe that the dependence of $\Delta E$ on constituent mass $M$ is very weak for the "exponential" parametrization. This is illustrated in Fig. 4 where the "exponential" parametrization (represented by convex lines) is plotted for two extreme constituent masses $M = 350$ and $M = 600$ MeV. The difference is no more as 150 MeV for realistic $m_s$.

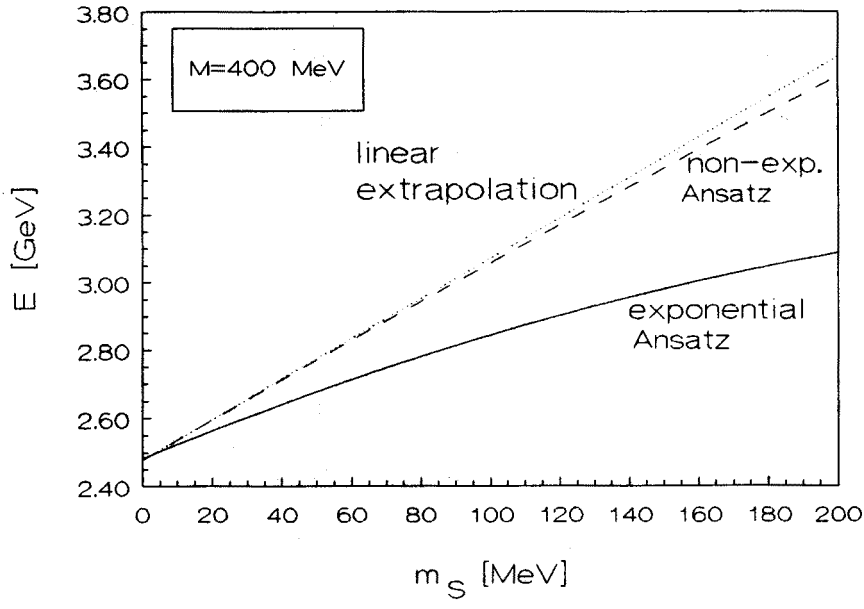


**Fig. 5.** $E$ **dependence on** $m_s$ **for** $M = 400$ **MeV in linear approximation (4.3) (short dash), full dependence with "non-exponential" parametrization (2.14) and "exponential" parametrization (4.7).**

## 5. Summary and conclusions

The purpose of this paper was to calculate the energy of the soliton [23] based on the specific SO(3) embedding in the SU(3) flavor group [18, 19]. We interpreted this energy $E_{\mathrm{dilambda}}$ as a mass of the dilambda state (or H), which consists of 6 quarks: uuddss [1]. Similarly to the solutions studied in the Skyrme model, H being a singlet state is not further split when the system is adiabatically rotated and then semiclassically quantized [18, 19]. Therefore, unlike in the case of hyperons [43, 44], the soliton mass $E_{\mathrm{dilambda}}$ *is equal* to the dilambda mass itself.

We have studied the behavior of $E_{\mathrm{dilambda}}$ with respect to model parameter $M$, *i.e.* the constituent quark mass and with respect to the current strange quark mass $m_s$. We have found that in the chiral limit $E_{\mathrm{dilambda}} \approx 2.5$ GeV with only slight dependence on $M$. The influence of $m_s$ has been studied first in a linear approximation. In a linear approximation the shift due to $m_s$ is calculated by assuming that the strange quark mass is small enough to apply Taylor expansion in the vicinity of $m_s = 0$. The increase of the H mass for $m_s = 156$ MeV is as big as 1 GeV for $M = 350$ MeV and decreases to 570 MeV for $M = 600$ MeV. For realistic $M$ the dilambda

mass is therefore shifted by about 40% — this is a signal that $m_s$, at least as far as total shift is concerned, cannot be treated as a small parameter. We have therefore decided to calculate the soliton mass with the non-zero strange quark mass in a nonlinear approximation where the singlet part of the mass matrix is treated exactly. In this nonlinear approach the chiral result is shifted by approximately 500 MeV for $m_s = 156$ MeV with only slight dependence on the constituent mass $M$. In short, our prediction for $E_{\text{dilambda}}$ reads:

$$E_{\text{dilambda}} \approx \underbrace{2.5 \text{ GeV}}_{\text{chiral}} + \underbrace{0.5 \text{ GeV}}_{m_s=156 \text{ MeV}} = 3 \text{ GeV}. \tag{5.1}$$

The above result was obtained in a variational approach. A full-scale self-consistent minimization of the energy functional (2.1) should in principle give predictions lower than Eq. (5.1), however from the experience with the *hedgehog* Ansatz we expect that our results are accurate to within a few percent.

In Ref. [23] the H mass was calculated for $M = 345$ MeV, a value dictated by the instanton model of the QCD vacuum. However, unlike in the present work, the energy of the continuum was calculated by means of the approximate *interpolation* formula and in the chiral limit the result read: $E_{\text{dilambda}} = 2.11$ GeV at $r_f = 1.1\,M$ and $r_g = 1.3\,M$. It has been already observed in the case of the *hedgehog* Ansatz that the *interpolation* formula is usually below the exact result. Also here for the SO(3) Ansatz the *interpolation* formula underestimates the exact result as well.

Before we come to the discussion of result (5.1), let us first motivate the nonlinear approach to the strange quark mass. The current quark mass matrix $m$ can be put into the following form:

$$\begin{bmatrix} m_u & 0 & 0 \\ 0 & m_d & 0 \\ 0 & 0 & m_s \end{bmatrix} = \mu_0\,\lambda_0 - \mu_8\,\lambda_8 - \mu_3\,\lambda_3\,, \tag{5.2}$$

where $\lambda_i$ are Gell-Mann SU(3) matrices ($\lambda_0 = \sqrt{2/3}\,\mathbf{1}$) and

$$\begin{aligned} \mu_0 &= \frac{1}{\sqrt{6}}(m_u + m_d + m_s)\,, \\ \mu_8 &= \frac{1}{2\sqrt{3}}(2\,m_s - m_u - m_d)\,, \\ \mu_3 &= \frac{1}{2}(m_u - m_d)\,. \end{aligned} \tag{5.3}$$

The three parameters $\mu_{0,8,3}$ are related to the strength of the chiral symmetry breaking, SU(3) breaking and isospin breaking respectively. In what

we call linear approach all quantities are expanded around the point $\mu_i = 0$. On the other hand the nonlinear treatment of $\mu_0$ corresponds to a picture in which the chiral symmetry breaking is diagonalized *exactly*, while the SU(3) breaking and the isospin breaking are still accounted for perturbatively (despite the fact that $\mu_0$ and $\mu_8$ are of the same order, *i.e.* $O(m_s)$, numerically $\mu_0 > \mu_8$). Let us remind that the perturbative expansion in $\mu_8$ has been successfully applied to calculate the hyperon splittings in the SU(3) $\chi$QM.

The two lambda threshold $E_{2\Lambda} = 2.23$ GeV is certainly below our result, both in the chiral limit and for the non-zero $m_s$. Should one therefore abandon the idea of producing a six quark state which would be stable with respect to strong interactions ? $\chi$QM, as well as other chiral models like the Skyrme model for instance, *overestimates* the absolute masses of hyperons [45]. Similarly to the case of the ordinary baryons we may therefore expect that our result for $E_{\mathrm{dilambda}}$ *overshoots* the would-be experimental result as well.

The energy of a given baryon belonging to representation R of the SU(3) flavor group (R=**8** or **10**) of spin $J$ ($J = {}^1/_2$ or ${}^3/_2$ respectively) is given by [43, 44, 46–48]:

$$M_{\mathrm{B}} = M_{\mathrm{cl}} + \Delta M_{\mathrm{cl}} + H_{\mathrm{SU(2)}} + H_{\mathrm{SU(3)}} + H_{\mathrm{br}}\,, \tag{5.4}$$

where

$$H_{\mathrm{SU(2)}} = \frac{J(J+1)}{2I_A}\,, \tag{5.5}$$

$$H_{\mathrm{SU(3)}} = \frac{C_2(\mathrm{SU(3)}) - J(J+1) - \frac{N_c^2}{12}}{2I_B}\,. \tag{5.6}$$

Here $I_{A,B}$ are certain moments of inertia calculable in the model, $C_2(\mathrm{SU(3)})$ is a quadratic Casimir operator, which should be evaluated for representation R, and $H_{\mathrm{br}}$ is a breaking piece responsible for splittings. $H_{\mathrm{br}}$ corresponds to $\mu_8\lambda_8$ in Eq. (5.2), whereas $\Delta M_{\mathrm{cl}}$ corresponds to $\mu_0\lambda_0$. $M_{\mathrm{cl}}$ is a classical soliton mass. As one can easily see from Eq. (5.4) $E_{\mathrm{hedgehog}} = M_{\mathrm{cl}} + \Delta M_{\mathrm{cl}}$ binds the hyperon masses from below. $H_{\mathrm{SU(2)}}$ and $H_{\mathrm{SU(3)}}$ are always positive; for the octet they are approximately equal to 60 MeV and 245 MeV respectively [43, 44]. $H_{\mathrm{br}}$ can be either positive or negative: for $\Lambda$ $H_{\mathrm{br}} \approx -40$ MeV. Therefore the $\Lambda$ mass is bigger than $E_{\mathrm{hedgehog}}$ by about 265 MeV. In Table V we display twice the energy $E_{\mathrm{hedgehog}}$ of the soliton calculated for the *hedgehog* Ansatz (1.2) for various constituent quark masses and various $m_s$ in the linear and nonlinear treatment. The results presented in Table V have been obtained by the selfconsistent minimization of the energy functional (2.1). For $M < 350$ MeV and $m_s$=0 and also for $M = 350$ MeV and $m_s \geq 100$ MeV no selfconsistent solution was found.

TABLE V

Twice soliton energy $E_{hedgehog}$ and $\sigma$ for *hedgehog* Ansatz of Eq. (1.2) for different constituent quark masses $M$ and bare strange quark masses $m_s$.

| $M$ [MeV] | $m_s$ [MeV] | $2\sigma$ | $2E_{\text{hedgehog}}$ [GeV] | |
|---|---|---|---|---|
| | | | linear | nonlinear |
| 350 | 0 | 6.54 | 2.53 | 2.53 |
| | 50 | | 2.86 | 2.78 |
| | 100 | | 3.18 | – |
| | 156 | | 3.55 | – |
| | 200 | | 3.84 | – |
| 400 | 0 | 6.03 | 2.51 | 2.51 |
| | 50 | | 2.81 | 2.74 |
| | 100 | | 3.11 | 2.91 |
| | 156 | | 3.45 | 3.07 |
| | 200 | | 3.71 | 3.18 |
| 500 | 0 | 4.92 | 2.43 | 2.43 |
| | 50 | | 2.68 | 2.64 |
| | 100 | | 2.92 | 2.79 |
| | 156 | | 3.20 | 2.94 |
| | 200 | | 3.42 | 3.04 |
| 600 | 0 | 4.23 | 2.35 | 2.35 |
| | 50 | | 2.56 | 2.54 |
| | 100 | | 2.77 | 2.67 |
| | 156 | | 3.01 | 2.79 |
| | 200 | | 3.19 | 2.89 |

The quantity $\sigma$ (defined in analogy with Eqs (4.2), (4.3)) displayed in the third column of Table V is related to the nucleon sigma-term $\Sigma$:

$$\Sigma = \frac{3}{4}(m_u + m_d)\, 2\sigma . \tag{5.7}$$

For $m_u + m_d = 12$ MeV $\Sigma = 9 \times 2\sigma$ MeV and varies with the constituent mass from 59 MeV to 38 MeV for $M = 350$ MeV and $M = 600$ MeV respectively. This dependence of $\Sigma$ points towards constituent quark masses of the order of 400 MeV, where the agreement with experimental value of 51 Mev is achieved.

Let us observe that twice the *hedgehog* mass, $2E_{\text{hedgehog}}$ is always bigger than the dilambda mass by a few tens MeV, both in chiral limit and off-chiral limit in both linear and nonlinear treatment. Within a percent accuracy the model predicts that

$$E_{\text{dilambda}} \approx 2\, E_{\text{hedgehog}} .$$

The two lambda threshold is about 530 MeV higher than $2E_{\text{hedgehog}}$ itself, therefore within the Chiral Quark Model dilambda is stable against strong

decays. The above result should be contrasted with the Skyrme model result, where $E_{\text{dilambda}}$ is comparable with $E_{\text{hedgehog}}$.

The whole discussion of the $m_s$ influence on the soliton mass was ment to show that actually both $B = 1$ and $B = 2$ solitons are affected by a nonzero strange quark mass in the same way, rather than to advocate the result obtained by the linear or nonlinear approach. That means that the conclusions concerning the stability of H in the chiral limit remain unchanged if we turn on the strange quark mass, irrespectively of the method (linear or nonlinear).

Let us finish by a remark concerning the cut-off function $\varphi(\tau)$. which is fixed by gradient expansion. Gradient expansion is a common procedure since it is technically not feasible to treat the fermion determinant up to all orders in $m$. However, in principle, even in the gradient expansion the effect of the singlet part of the current quark mass can be treated nonlinearly in close analogy to the soliton case discussed above. Indeed, such an approach consists in shifting a constituent quark mass by $m_s/3$ for all quarks. This effect has a negligible influence on our results. It amounts to a change of the cut-off parameters through Eqs (2.6), (2.7) and, as we have checked numerically, it diminishes the mass of the soliton by at most 10% both in $B = 2$ and $B = 1$ sector. The conclusions concerning the stability of H remain therefore unchanged.

While the overestimation of the absolute masses seems to be a common disease of chiral models there are some corrections, which we did not take into account, which lower the soliton mass. In Ref. [49] one gluon correction was calculated and shown to be negative, but too large to trust the perturbative expansion in $\alpha_{\text{strong}}$. Subtraction of the *rotational bands* might be also another way out [44]. Let us finally mention the Casimir energy discussed recently in Ref. [50]. It is certainly beyond the scope of this paper to discuss this problem in detail, we only mention those possibilities in order to emphasize that we are not at the end of our way towards the understanding of the predictions for the absolute values of the hadronic masses in chiral models.

This work was partly sponsored by *Studienstiftung des deutschen Volkes* (P.S.). We would like to thank D.I. Diakonov, K. Goeke, Th. Meissner, V.Yu. Petrov and P.V. Pobylitsa for useful discussions at various stages of this work. Z.D. thanks the Bochum Theory Group for hospitality during his stay in Germany.

## Appendix A

*Spherical isospinors for* SO(3) *symmetry group*

In this appendix we collect formulae for spinors which diagonalize Dirac equation (2.2). In order to get a state with a given grand-spin $K$ we first construct two two-component spinors $\Omega^{\pm}_{J,J_3}$, where $\boldsymbol{J} = \boldsymbol{S} + \boldsymbol{L}$ . The upper superscript refers to the eigenvalue $L$ which for given $J$ and spin $^1/_2$ can be either $L = J - {}^1/_2$ or $L = J + {}^1/_2$

$$\Omega^{(-)}_{J,J_3} = \frac{1}{\sqrt{2J}} \begin{bmatrix} \sqrt{J+J_3}\; Y_{J-\frac{1}{2},J_3-\frac{1}{2}} \\ \sqrt{J-J_3}\; Y_{J-\frac{1}{2},J_3+\frac{1}{2}} \end{bmatrix},$$

$$\Omega^{(+)}_{J,J_3} = \frac{1}{\sqrt{2J+2}} \begin{bmatrix} -\sqrt{J+1-J_3}\, Y_{J+\frac{1}{2},J_3-\frac{1}{2}} \\ \sqrt{J+1+J_3}\, Y_{J+\frac{1}{2},J_3+\frac{1}{2}} \end{bmatrix}. \tag{A.1}$$

Next we construct six 6-component spinors $\Xi^{(\pm 0,\pm)}_{K,K_3}$. Here the second superscript, as in the case of $\Omega$, corresponds to two ways spin and angular momentum can be coupled to form given $J$, and the first superscript refers to three ways $J$ and SO(3) "momentum" $\Lambda = 1$ can be coupled to form given (half-integer) grand-spin $K$:

$$\Xi^{(-,j)}_{K,K_3} = N^{(-)} \begin{bmatrix} \sqrt{(K+K_3-1)(K+K_3)}\, \Omega^{(j)}_{K-1,K_3-1} \\ \sqrt{2(K+K_3)(K-K_3)}\, \Omega^{(j)}_{K-1,K_3} \\ \sqrt{(K-K_3-1)(K-K_3)}\, \Omega^{(j)}_{K-1,K_3+1} \end{bmatrix},$$

$$\Xi^{(0,j)}_{K,K_3} = N^{(0)} \begin{bmatrix} -\sqrt{(K+K_3)(K-K_3+1)}\, \Omega^{(j)}_{K,K_3-1} \\ \sqrt{2}K_3\, \Omega^{(j)}_{K,K_3} \\ \sqrt{(K-K_3)(K+K_3+1)}\, \Omega^{(j)}_{K,K_3+1} \end{bmatrix},$$

$$\Xi^{(+,j)}_{K,K_3} = N^{(+)} \begin{bmatrix} \sqrt{(K-K_3+1)(K-K_3+2)}\, \Omega^{(j)}_{K+1,K_3-1} \\ -\sqrt{2(K-K_3+1)(K+K_3+1)}\, \Omega^{(j)}_{K+1,K_3} \\ \sqrt{(K+K_3+1)(K+K_3+2)}\, \Omega^{(j)}_{K+1,K_3+1} \end{bmatrix}, \tag{A.2}$$

where normalization factors are given by:

$$N^{(-)} = \frac{1}{\sqrt{2K(2K-1)}},$$

$$N^{(0)} = \frac{1}{\sqrt{2K(K+1)}},$$

$$N^{(+)} = \frac{1}{\sqrt{2(K+1)(2K+3)}}$$

and $j = -,\ +$.

In order to derive spherical Dirac equation we need the following relations:

$$\begin{aligned}
\boldsymbol{n}\cdot\boldsymbol{\Lambda}\,\Xi^{(i,j)} &= \frac{1}{2K+1+i}\left(i\,\Xi^{(i,-j)}\right.\\
&\quad\left.-\frac{1}{\sqrt{2}}\sqrt{(2K+1-i)(2K+1+2i)}\,\Xi^{(0,j)}\right),\\
\boldsymbol{n}\cdot\boldsymbol{\Lambda}\,\Xi^{(0,j)} &= \frac{1}{2K(K+1)}\,\Xi^{(0,-j)}\\
&\quad-\frac{\sqrt{K(2K+3)}}{2(K+1)}\,\Xi^{(+,j)}-\frac{\sqrt{(K+1)(2K-1)}}{2K}\,\Xi^{(-,j)},\\
\boldsymbol{L}\cdot\boldsymbol{\sigma}\,\Xi^{(i,j)} &= -\,j\,(K+\frac{1}{2}+i+j)\,\Xi^{(i,j)},\\
\boldsymbol{n}\cdot\boldsymbol{\sigma}\,\Xi^{(i,j)} &= -\,\Xi^{(i,-j)},
\end{aligned}\tag{A.3}$$

where we have suppressed subscripts $K, K_3$. Here $i, j = \pm 1$ , $\vec{\sigma}$ matrices are related to the spin operator.

## Appendix B

### *Radial Dirac equation*

The Dirac equation (2.2) can be written in a matrix form:

$$\begin{bmatrix} \epsilon_l & i\boldsymbol{\sigma}\cdot\boldsymbol{\partial} \\ i\boldsymbol{\sigma}\cdot\boldsymbol{\partial} & \epsilon_l \end{bmatrix}\psi_l =$$

$$\begin{bmatrix} 2b_1(\boldsymbol{n}\cdot\boldsymbol{\Lambda})+4b_2(\boldsymbol{n}\cdot\boldsymbol{\Lambda})^2+b_3 & -i(2a_1(\boldsymbol{n}\cdot\boldsymbol{\Lambda})-4a_2(\boldsymbol{n}\cdot\boldsymbol{\Lambda})^2+a_3) \\ i(2a_1(\boldsymbol{n}\cdot\boldsymbol{\Lambda})-4a_2(\boldsymbol{n}\cdot\boldsymbol{\Lambda})^2+a_3) & -2b_1(\boldsymbol{n}\cdot\boldsymbol{\Lambda})-4b_2(\boldsymbol{n}\cdot\boldsymbol{\Lambda})^2-b_3 \end{bmatrix}\psi_l,\tag{B.1}$$

where $\boldsymbol{\partial} \equiv \partial/(M\partial\boldsymbol{r})$, and

$$\begin{aligned}
a_1 &= \tfrac{1}{2}\cos\tfrac{g}{3}\sin f, & b_1 &= -\tfrac{1}{2}\sin\tfrac{g}{3}\sin f,\\
a_2 &= -\tfrac{1}{4}\left(\sin\tfrac{g}{3}\cos f+\sin\tfrac{2g}{3}\right), & b_2 &= \tfrac{1}{4}\left(\cos\tfrac{g}{3}\cos f-\cos\tfrac{2g}{3}\right),\\
a_3 &= -\sin\tfrac{2g}{3}, & b_3 &= \cos\tfrac{2g}{3}.
\end{aligned}\tag{B.2}$$

In Sec. 4 we discuss non-linearities caused by finite $m_s$. Then one should replace $b_3$ by

$$b_3 = \cos\frac{2g}{3}+\frac{1}{3}m_s.\tag{B.3}$$

Equation (B.1) becomes block-diagonal in basis (2.12), each block being a $12 \times 12$ dimensional matrix, so that the different values of $K$ do not mix. As mentioned already in section 2 in the vacuum sector equation (B.1) splits further into three $4 \times 4$ subequations. Accordingly we decompose 12-dimensional vector $\Psi_{K,n}(x)$ into three 4-component vectors $\Psi^{\pm\,0}_{K,n}$:

$$\Psi_{K,n} = \begin{bmatrix} \Psi^{+}_{K,n} \\ \Psi^{0}_{K,n} \\ \Psi^{-}_{K,n} \end{bmatrix}, \tag{B.4}$$

From now on the subscript $n$ enumerating eigenenergies as well as $x$-dependence will be suppressed.

Elements of $\Psi^{i}_{K}$ (with $i = \pm, 0$) are related to functions $G$ and $F$ defined in Eq. (2.12):

$$\Psi^{i}_{K} = \begin{bmatrix} F^{K}_{(i,+)} \\ G^{K}_{(i,-)} \\ G^{K}_{(i,+)} \\ F^{K}_{(i,-)} \end{bmatrix}. \tag{B.5}$$

In the same way matrices $N$, $C_K$ and $H_K$ can be split into 9 blocks of $4 \times 4$ matrices, *e.g.*:

$$H = \begin{bmatrix} H^{(+,+)} & H^{(+,0)} & H^{(+,-)} \\ H^{(0,+)} & H^{(0,0)} & H^{(0,-)} \\ H^{(-,+)} & H^{(-,0)} & H^{(-,-)} \end{bmatrix}, \tag{B.6}$$

where we have suppressed subscript $K$.

For $N$ and $C$ only diagonal submatrices are non-zero:

$$N^{(\pm,\pm)} = N^{(0,0)} = \begin{bmatrix} 0 & 1 & & \\ -1 & 0 & & \\ & & 0 & -1 \\ & & 1 & 0 \end{bmatrix} \tag{B.7}$$

and

$$C^{(\pm,\pm)} = \begin{bmatrix} 0 & -K + \frac{1}{2} \mp 1 & & \\ -K - \frac{3}{2} \mp 1 & 0 & & \\ & & 0 & K - \frac{1}{2} \pm 1 \\ & & K + \frac{3}{2} \pm 1 & 0 \end{bmatrix}, \tag{B.8}$$

and $C^{(0,0)} = {}^{1}\!/_{2}(C^{(+,+)} + C^{(-,-)})$.

Now we will specify matrix $H$. Matrix $H$ is real and symmetric, therefore

$$H^{(i,j)}_{a,b} = H^{(j,i)}_{b,a}.$$

Also submatrices $H^{(i,j)}$ are symmetric:

$$H^{(i,j)}_{a,b} = H^{(i,j)}_{b,a}.$$

They are also symmetric with respect to the second diagonal, namely:

$$H^{(i,j)}_{a,5-b} = H^{(i,j)}_{b,5-a},$$

where $a, b = 1, \ldots, 4$. Moreover:

$$\begin{aligned} H^{(i,j)}_{2,2} &= -H^{(i,j)}_{1,1}, \\ H^{(i,j)}_{2,3} &= -H^{(i,j)}_{1,4}, \end{aligned} \tag{B.9}$$

It is therefore enough to specify the following elements of $H$:

$$\begin{aligned}
H^{(+,+)}_{1,1} &= b_3 + b_2 \tfrac{2K+1}{K+1}, & H^{(+,+)}_{1,2} &= -a_1 \tfrac{1}{K+1}, \\
H^{(+,+)}_{1,3} &= -a_3 + a_2 \tfrac{2K+1}{K+1}, & H^{(+,+)}_{1,4} &= b_1 \tfrac{1}{K+1}, \\
H^{(0,0)}_{1,1} &= b_3 + b_2 \tfrac{4K^2+4K-1}{K(K+1)}, & H^{(0,0)}_{1,2} &= -a_1 \tfrac{1}{K(K+1)}, \\
H^{(0,0)}_{1,3} &= -a_3 + a_2 \tfrac{4K^2+4K-1}{K(K+1)}, & H^{(0,0)}_{1,4} &= b_1 \tfrac{1}{K(K+1)}, \\
H^{(-,-)}_{1,1} &= b_3 + b_2 \tfrac{2K+1}{K}, & H^{(-,-)}_{1,2} &= a_1 \tfrac{1}{K}, \\
H^{(-,-)}_{1,3} &= -a_3 + a_2 \tfrac{2K+1}{K}, & H^{(-,-)}_{1,4} &= -b_1 \tfrac{1}{K}, \\
H^{(+,0)}_{1,1} &= -b_1 \tfrac{\sqrt{K(2K+3)}}{K+1}, & H^{(+,0)}_{1,2} &= -a_2 \tfrac{\sqrt{K(2K+3)}}{K(K+1)}, \\
H^{(+,0)}_{1,3} &= a_1 \tfrac{\sqrt{K(2K+3)}}{K+1}, & H^{(+,0)}_{1,4} &= -b_2 \tfrac{\sqrt{K(2K+3)}}{K(K+1)}, \\
H^{(0,-)}_{1,1} &= -b_1 \tfrac{\sqrt{(K+1)(2K-1)}}{K}, & H^{(0,-)}_{1,2} &= a_2 \tfrac{\sqrt{(K+1)(2K-1)}}{K(K+1)}, \\
H^{(0,-)}_{1,3} &= a_1 \tfrac{\sqrt{(K+1)(2K-1)}}{K}, & H^{(0,-)}_{1,4} &= b_2 \tfrac{\sqrt{(K+1)(2K-1)}}{K(K+1)}, \\
H^{(+,-)}_{1,1} &= b_2 \sqrt{\tfrac{(2K+3)(2K-1)}{K(K+1)}}, & H^{(+,-)}_{1,2} &= 0, \\
H^{(+,-)}_{1,3} &= a_2 \sqrt{\tfrac{(2K+3)(2K-1)}{K(K+1)}}, & H^{(+,-)}_{1,4} &= 0.
\end{aligned} \tag{B.10}$$

## Appendix C

*Discrete basis*

In Section 2 we introduced finite basis which was subsequently used to diagonalize Eq. (2.13). Let us split the 12-dimensional component vector $\Phi_K$ into three 4-component vectors $\overset{\pm}{\Phi}{}^{0}_{K}$:

$$\Phi_K = \begin{bmatrix} \Phi^+_K \\ \Phi^0_K \\ \Phi^-_K \end{bmatrix}. \tag{C.1}$$

In order to construct the basis vectors (2.15) it is enough to specify the form of, say, $\Phi^+_K$ with $\Phi^-_K = 0$ and $\Phi^0_K = 0$, then $\Phi^0_K$ with $\Phi^+_K = 0$ and $\Phi^-_K = 0$, and finally $\Phi^-_K$ with $\Phi^+_K = 0$ and $\Phi^0_K = 0$. These 4-dimensional vectors for given $K$ are given in terms of radial Bessel functions:

$$\overset{\pm}{\Phi}{}^{0}_{K,1} = \begin{bmatrix} j_{K+\frac{1}{2}+j}(kx) \\ 0 \\ 0 \\ 0 \end{bmatrix}, \quad \overset{\pm}{\Phi}{}^{0}_{K,2} = \begin{bmatrix} 0 \\ j_{K-\frac{1}{2}+j}(kx) \\ 0 \\ 0 \end{bmatrix},$$

$$\overset{\pm}{\Phi}{}^{0}_{K,3} = \begin{bmatrix} 0 \\ 0 \\ j_{K+\frac{1}{2}+j}(kx) \\ 0 \end{bmatrix}, \quad \overset{\pm}{\Phi}{}^{0}_{K,4} = \begin{bmatrix} 0 \\ 0 \\ 0 \\ j_{K-\frac{1}{2}+j}(kx) \end{bmatrix}. \tag{C.2}$$

where $j = 1, -1, 0$ for superscript $+, -$ and 0 respectively.

In this notation the boundary conditions (2.18) read:

$$j_{K-\frac{1}{2}+j}(k^j_n D) = 0. \tag{C.3}$$

Our basis is orthogonal due to the relation:

$$\int_0^D j_\nu(k_n) j_\nu(k_m)\, x^2\, dx = \int_0^D j_{\nu\pm1}(k_n) j_{\nu\pm1}(k_m)\, x^2\, dx$$

$$= \delta_{n,m} \frac{D^3}{2} j'_\nu(k_n D), \tag{C.4}$$

but *only* if $k_n$ is a solution of the equation:

$$j_\nu(k_n D) = 0. \tag{C.5}$$

As seen from Eq. (C.2) Bessel functions present in our basis have indices $\nu$ ranging from $K-{}^3/_2$ to $K+{}^3/_2$ and therefore, since there is no orthogonality condition similar to (C.5) for $j_{\nu+2}$, we are not able to construct an orthogonal basis with the single boundary condition (C.5). Instead, in order to satisfy orthogonality of basis states, we impose three different boundary conditions (C.3).

## REFERENCES


[1] R.L. Jaffe, *Phys. Rev. Lett.* **38**, 195 (1977).
[2] A. Caroll *et al.*, *Phys. Rev. Lett.* **41**, 777 (1978) 777.
[3] G.B. Franklin, *Nucl. Phys.* **A450**, 117c (1986).
[4] P. Barnes, Perspectives in strange particle physics, In *Springer Proceedings in Physics 26, The Elementary Structure of Matter*, eds N. Boccara, J.-M. Richard, E. Aslanides, Springer Verlag, 1987, p. 292.
[5] S. Aoki *et al.*, *Phys. Rev. Lett.* **65**, 1729 (1990).
[6] J. Sandweiss *et al.*, Brookhaven AGS Experiment E864.
[7] P.J. Mulders, A.T. Aerts, J.J. de Swart, *Phys. Rev.* **D21**, 2653 (1980).
[8] K.F. Liu, C.W. Wong, *Phys. Lett.* **113B**, 1 (1982).
[9] P.J. Mulders, A.W. Thomas, *J. Phys. G* **9**, 1159 (1983).
[10] A.T. Aerts, J. Rafelski, *Phys. Lett.* **148B**, 337 (1984).
[11] J.L. Rosner, *Phys. Rev.* **D33**, 2043 (1986).
[12] P. MacKenzie, H.B. Thacker, *Phys. Rev. Lett.* **55**, 2539 (1985).
[13] Y. Iwasaki, T. Yoshié, T. Tsubai, *Phys. Rev. Lett.* **60**, 1371 (1988).
[14] M. Oka, K. Shimizu, K. Yazaki, *Phys. Lett.* **130B**, 365 (1983).
[15] M. Oka, K. Shimizu, K. Yazaki, *Nucl. Phys.* **A464**, 700 (1987).
[16] U. Straub *et al.*, *Phys. Lett.* **200B**, 241 (1988).
[17] U. Straub *et al.*, *Nucl. Phys.* **A438**, 686 (1988).
[18] A.P. Balachandran *et al.*, *Phys. Rev. Lett.* **52**, 887 (1984).
[19] A.P. Balachandran *et al.*, *Nucl. Phys.* **B256**, 525 (1985).
[20] R.L. Jaffe, C. L. Korpa, *Nucl. Phys.* **B258**, 468 (1985).
[21] S.A. Yost, C. R. Nappi, *Phys. Rev.* **D32**, 816 (1985).
[22] N. Aizawa, M. Hirata, *Prog. Theor. Phys.* **86**, 429 (1991).
[23] D.I. Diakonov, V.Yu. Petrov, P.V. Pobylitsa, M. Praszałowicz, *Phys. Rev.* **D39**, 3509 (1989).
[24] M.S. Birse, M. K. Banerjee, *Phys. Lett.* **136B**, 294 (1984).
[25] G. Ripka, S. Kahana, *Phys. Rev.* **D36**, 1233 (1987).
[26] D.I. Dyakonov, V.Yu. Petrov, P.V. Pobylitsa, *Phys. Lett.* **205B**, 372 (1988).
[27] D.I. Dyakonov, V.Yu. Petrov, P.V. Pobylitsa, *Nucl. Phys.* **B306**, 809 (1988).
[28] H. Reinhardt, R. Wünsch, *Phys. Lett.* **215B**, 577 (1988).
[29] Th. Meissner, F. Grümmer, K. Goeke, *Phys. Lett.* **227B**, 296 (1989).
[30] Th. Meissner, F. Grümmer, K. Goeke, *Ann. Phys. (NY)* **202**, 297 (1990).
[31] M. Wakamatsu, *Ann. Phys.* **193**, 287 (1989).
[32] Y. Nambu, G. Jona-Lasinio, *Phys. Rev.* **124**, 246 (1961).

[33] D.I. Dyakonov, V.Yu. Petrov, *Nucl. Phys.* **B245**, 259 (1984).
[34] D.I. Dyakonov, V.Yu. Petrov, *Nucl. Phys.* **B272**, 457 (1986).
[35] J. Schwinger, *Phys. Rev.* **82**, 664 (1951).
[36] D.I. Diakonov, V.Yu. Petrov, M. Praszałowicz, *Nucl. Phys.* **B323**, 53 (1989).
[37] H. Reinhardt, *Nucl. Phys.* **A503**, 825 (1989).
[38] M. Wakamatsu, H. Yoshiki, *Nucl. Phys.* **A524**, 561 (1991).
[39] M. Praszałowicz, G. Valencia, *Nucl. Phys.* **B341**, 27 (1990).
[40] E. Ruiz Arriola, *Phys. Lett* **253B**,??? (1991).
[41] T.H.R. Skyrme, *Proc. R. Soc.* **A260**, 127 (1961).
[42] G.S. Adkins, C.R. Nappi, E. Witten, *Nucl. Phys.* **B228**, 552 (1983).
[43] A. Blotz, D.I. Diakonov, K. Goeke, N.W. Park, V. Petrov, P.V. Pobylitsa, *Phys. Lett.* **B287**, 29 (1992).
[44] A. Blotz, D.I. Diakonov, K. Goeke, N.W. Park, V. Petrov, P.V. Pobylitsa, *Nucl. Phys.* **A555**, 765 (1993).
[45] M. Praszałowicz, *Acta. Phys. Pol.* **B22**, 525 (1991).
[46] E. Guadagnini, *Nucl. Phys.* **B236**, 35 (1984).
[47] M. Praszałowicz, *Phys. Lett.* **158B**, 264 (1985).
[48] S. Jain, S. R. Wadia, *Nucl. Phys.* **B258**, 713 (1985).
[49] D.I. Diakonov, J. Jaenicke, M.V. Polyakov, Gluon exchange corrections to the nucleon mass in the chiral theory, St. Petersburg preprint 1738, 1991.
[50] B. Moussalam, D. Kalafatis, *Phys. Lett.* **B272**, 196 (1991).